Proc. Natl. Acad. Sci. USA
Vol. 93, pp. 5975–5979, June 1996
Applied Mathematics

Kinetics of self-assembling microtubules: An "inverse problem" in biochemistry

HENRIK FLYVBJERG*†‡, ELMAR JOBS*, AND STANISLAS LEIBLER†

*Höchstleistungsrechenzentrum, Forschungszentrum Jülich, D-52425 Jülich, Germany; and †Departments of Physics and Molecular Biology, Princeton University, Princeton, NJ 08544-0708

Communicated by Michael E. Fisher, University of Maryland, College Park, MD, January 31, 1996 (received for review August 17, 1995)

ABSTRACT **Experimental time series for a nonequilibrium reaction may in some cases contain sufficient data to determine a unique kinetic model for the reaction by a systematic mathematical analysis. As an example, a kinetic model for the self-assembly of microtubules is derived here from turbidity time series for solutions in which microtubules assemble. The model may be seen as a generalization of Oosawa's classical nucleation–polymerization model. It reproduces the experimental data with a four-stage nucleation process and a critical nucleus of 15 monomers.**

In physics there is a so-called *inverse problem:* Particles are scattered off each other with various energies, and from the scattering data one tries to deduce the interaction potential between the particles. This problem has been well studied, and the mathematical requirements for existence and uniqueness of a solution are understood (1, 2).

In chemistry or biochemistry one can formulate an analogous inverse problem: what does it take to determine a reaction mechanism from the reaction's products? It is well known that one cannot find a unique mechanism from a steady-state kinetic analysis (3). Non-steady-state situations reveal more information, however. In this article, it is shown for a specific case how it is possible, with minimal simplifying assumptions, to derive a unique kinetic model from reaction data.

The case in question is an example of biological self-assembly, the spontaneous assembly of *microtubules.* The self-assembly of these protein fibers can be reproduced *in vitro* with purified tubulin and is an example of a far-from-equilibrium reaction. Under appropriate conditions, tubulin spontaneously assembles to form the cylindrical five-step helical "crystal lattice" constituting a microtubule. This symmetry of microtubules makes them simpler, and hence more susceptible to quantitative modeling, than many other self-assembling biological structures of interest.

An example of available data is shown in Fig. 1. The plotting symbols are experimental time series for the *turbidity* (A) of 13 different solutions of tubulin in which microtubules grow in presence of glycerol (4). The turbidity is a simple and precise physical measure of the amount of tubulin that has polymerized at any given time during assembly (see below). These time series define our inverse problem: we assume that they all resulted from the same assembly pathway, initiated with different initial concentrations, and try to find that pathway. The curves through the data points in Fig. 1 are *theoretical* time series resulting from a kinetic model which we have derived from the experimental data—i.e., an assembly model that solves the inverse problem.

The model found generalizes the classical model by Oosawa and coworkers (5–7). It is analytically soluble despite its highly nonlinear nature. More importantly, although a specific reaction is analyzed, the methods used here are generally applicable.

The main steps leading to the derivation of the unique assembly kinetics may be summarized as follows. (*i*) We analyzed the overall properties of the time series by looking for so-called *phenomenological scaling.* This property means that the individual time series is fully characterized by one characteristic turbidity scale and by one characteristic time scale, while its overall behavior is common to all the time series. This kind of simple behavior can be expected in particular from any process that consists of, or is dominated by, a single mechanism. The time series were found to scale to a good approximation (see Fig. 3).

(*ii*) We considered the dependence of the characteristic time on the characteristic turbidity. Both were read off the experimental time series, so their relationship could be found without knowledge of the assembly kinetics. We found a remarkably simple and robust relationship—namely, that the characteristic time is inversely proportional to the third power of the final turbidity (see Fig. 4).

(*iii*) We took these results to indicate that a kinetic model based on a single path of assembly would be adequate to describe the experimental data. We wrote down a generic model with a single assembly pathway and demanded that its solutions scale with a characteristic time that is inversely proportional to the third power of the initial concentration, which for its part, we argued, is proportional to the final turbidity. We found that these requirements *uniquely determine* the model up to the number of assembly steps in it, and the values of the rate constants for these steps.

(*iv*) We analyzed the initial growth of the time series and found them to grow with time to the fifth power (see Fig. 6). Again, the precision with which this power turns out to be integer supports our assumption that the underlying kinetics is sufficiently simple to reveal itself in the time series being analyzed. Specifically, this result tells us that a stable nucleus for polymerization is created in four steps. Thus the kinetic model was uniquely determined up to four rate constants.

(*v*) We solved the kinetic model exactly up to a single integral. The model is described by five coupled nonlinear first-order differential equations in time, but because of their scaling properties they can nevertheless be solved.

(*vi*) We fitted the solutions to the experimental time series, using the four rate constants as fitting parameters. Three of these rate constants set the rates for similar processes and turned out to have identical values when fitted to the data. So we might as well *assume* those three rate constants to be equal and work with a two-parameter theory. That theory is the one fitted to the data in Fig. 1.

Phenomenological Data Analysis

The experimental time series shown in Fig. 1 all have similar sigmoid shapes. We therefore ask whether they differ only

The publication costs of this article were defrayed in part by page charge payment. This article must therefore be hereby marked "*advertisement*" in accordance with 18 U.S.C. §1734 solely to indicate this fact.

‡Permanent address: Department of Optics and Fluid Dynamics, Ris National Laboratory, DK-4000 Roskilde, Denmark.

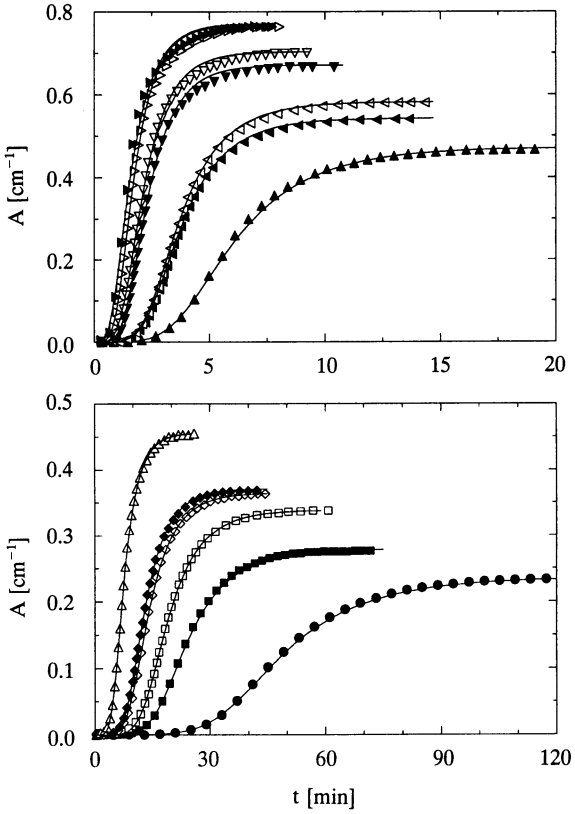

FIG. 1. Turbidity versus time of tubulin solution in which a temperature jump from 0 to 37°C at time 0 has induced microtubules to self-assemble. Plotting symbols show the turbidity time series for different initial concentrations of tubulin as measured by Voter and Erickson (4). [Of the 16 time series shown in figures 5 and 9 of ref. 4 we have left out three with slowest rates of assembly here because they were distinctly anomalous compared to the rest when analyzed as here. The properties of tubulin are known to change during experiments lasting as long as the slowest assemblies in ref. 4.] Fully drawn curves show the two-parameter fits to experimental data of theoretical turbidity series derived in this article.

through different overall time and turbidity scales. If this is the case, they are said to *scale,* meaning all of them can be described by a *single* function f as

$$A(t; A_\infty) = A_\infty f[t/t_0(A_\infty)], \qquad [1]$$

a property that obviously would reduce the task of modeling significantly. In Eq. **1** we distinguish the 13 time series and corresponding characteristics times, t_0, by the asymptotic value, A_∞, of the individual time series. This asymptotic value is easily determined from the data, and the relationship (Eq. **1**) is more easily determined by plotting A/A_∞ against t with double-log axis, since Eq. **1** implies that

$$\log(A/A_\infty) = g(\log t - \log t_0), \qquad [2]$$

where $g(x) = \log[f(\exp x)]$. Eq. **2** shows that if scaling is satisfied, different time series fall on curves that are identical, apart from being shifted horizontally along the log t axis relatively to each other.

In Fig. 2 the series are plotted this way and do seem to be identical up to a translation along the log t axis. To test for this last property, we read the so-called *tenth time,* t_0, off Fig. 2 for each time series and replotted the series as A/A_∞ against t/t_0 (see Fig. 3). The tenth time is the time when a series has reached one tenth of its final value. The choice of one tenth is conventional (4) and convenient for our purpose since we can easily obtain the tenth time with precision from Fig. 2. [In principle other definition (e.g., half time) could be used and would lead to the same results.]

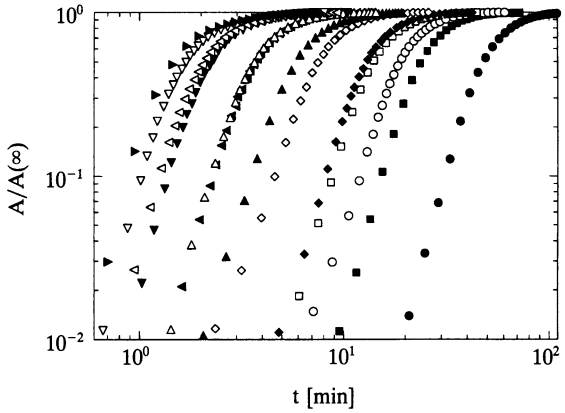

FIG. 2. Same data as in Fig. 1, plotted as $A(t)/A_\infty$ against time t using double-log axis.

Fig. 3 shows that the relationship in Eq. **1** does indeed hold to a high degree: the different time series fall on a single curve to a good approximation. The curve drawn through the data points is the graph of f which results from the theory developed below. This scaling property of the time series indicates that the underlying reaction mechanism is relatively simple.

The values for t_0, which we read off Fig. 2, are plotted against the corresponding values for A_∞ in Fig. 4. This figure shows quite convincingly that

$$t_0 \propto A_\infty^{-3}. \qquad [3]$$

This relationship is surprisingly simple. Like the scaling property, it indicates that a single mechanism is responsible for the assembly reaction observed, even though the total amount of tubulin polymerized in these reactions varies by a factor larger than 3, and their time scales by a factor larger than 30. Both the scaling property (Eq. **1**) and the power-law dependence (Eq. **3**) are of a precise mathematical form. Thus, without use of any theory whatsoever, our phenomenological analysis of the data has revealed mathematical demands on a model describing the data.

Models

Voter and Erickson (4) considered three theoretical models for their experimental time series: (*i*) the classical model by

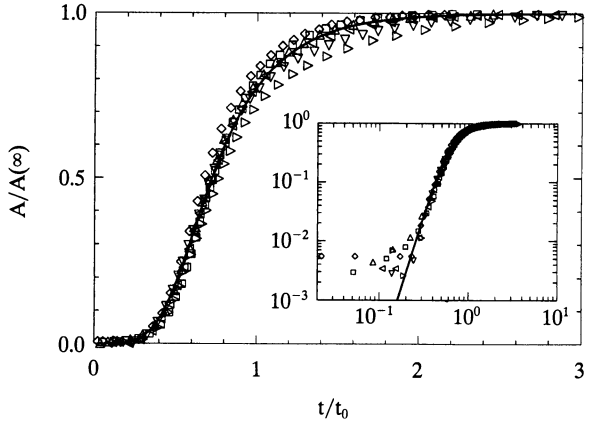

FIG. 3. Experimental data shown with open symbols in Fig. 1, replotted here as A/A_∞ against t/t_0, demonstrating data collapse. Fully drawn curve shows the two-parameter fit of theoretical turbidity to experimental data as described in the section *Rate Constants.* (*Inset*) Same data plotted with double-log axis.

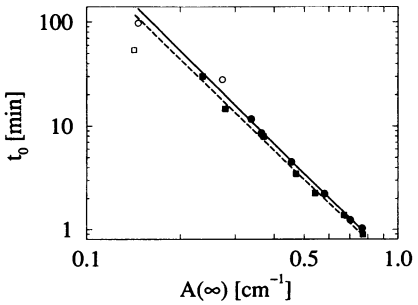

FIG. 4. Double-log plot of $t_0(A_\infty)$ versus A_∞. Circular symbols show results from figure 5 in ref. 4. The full straight line is a fit to the six filled round symbols, which correspond to the time series shown in Fig. 1 with open symbols. Its slope is -2.97 ± 0.05. Square symbols show results from figure 9 of ref. 4. The dashed straight line is a fit to the seven filled square symbols, which correspond to the time series shown in Fig. 1 with filled symbols. Its slope is -2.90 ± 0.09. The intercepts of the two straight lines with the second axis do not differ significantly, and give the constant of proportionality in Eq. **3** as 0.44 ± 0.03 min/cm^3.

Oosawa and coworkers (5–7), which is the simplest possible theory describing nucleation followed by polymerization [experimental results for the spontaneous self-assembly of *actin filaments,* which are relatively simple helical polymers, are fitted perfectly by this model (8)]; (*ii*) a double-nucleation model devised for the spontaneous polymerization of *deoxy sickle hemoglobin* (9); and (*iii*) a model for two-dimensional nucleation and polymerization inspired by the geometrical form of microtubules. Neither of these models described the time series well (4).

In view of this, we formulated a *generic* class of *phenomenological* models that describe the formation of a nucleus through *any* sequence of intermediate stages (Fig. 5). In principle, several different paths of assembly may contribute simultaneously to the formation of microtubules. If this is the case, it is hardly possible to separate and determine these paths from the turbidity time series alone. We therefore tentatively assumed that there is only one path for self-assembly (see ref. 10), and found that this assumption was confirmed by the results it lead us to. We also assumed that every stage in this path is connected to the next stage by addition of monomers only. This assumption is very reasonable because the monomer concentration greatly exceeds any other concentration throughout the nucleation process. With these assumptions, we could write down a generic set of kinetic equations describing the assembly process.

Let c denote the monomer concentration, c_i the number concentration of the ith relatively stable intermediate assembly product, n_i the number of monomers added to this product to form the $(i + 1)$th intermediate assembly product, k the number of different, successive intermediate products—i.e., k is the number of intermediate assembly stages of the nucleus—and ν the number concentration of nuclei, including such on which microtubules have grown. Let M denote the amount of mass polymerized to microtubules, discounting the mass in nuclei and intermediate assembly products, since the latter do not contribute to the turbidity. With this notation, and f_i, b_i, and d_i denoting forwards, backwards, and disintegration rate-constants, respectively, the kinetic equations are

$$dc_1/dt = f_0 c^{n_0} - f_1 c^{n_1} c_1 + b_2 c_2 - d_1 c_1, \quad [4]$$

$$dc_i/dt = f_{i-1} c^{n_{i-1}} c_{i-1} - f_i c^{n_i} c_i - b_i c_i + b_{i+1} c_{i+1} - d_i c_i \quad \text{for } 2 \le i \le k, \quad [5]$$

$$d\nu/dt = f_k c^{n_k} c_k, \quad [6]$$

$$dM/dt = f_{k+1} c \nu. \quad [7]$$

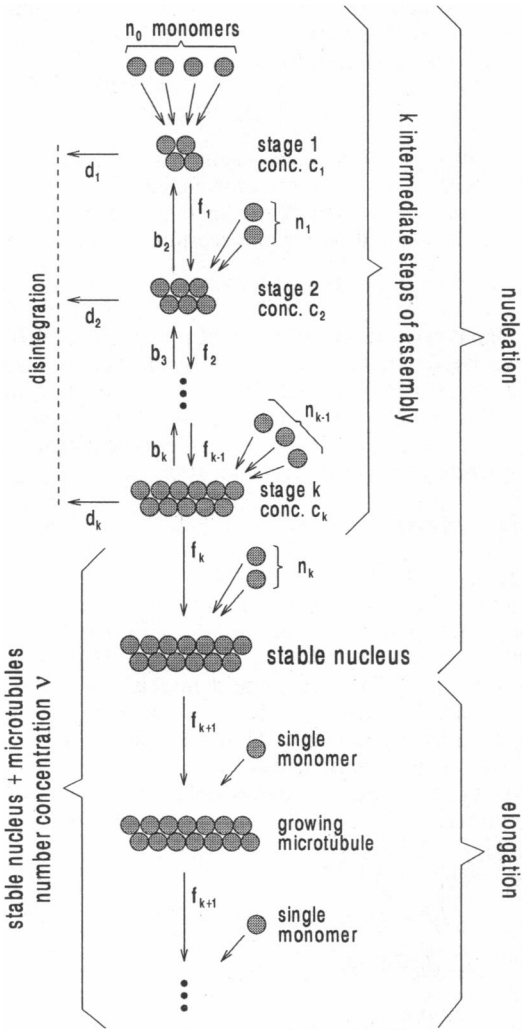

FIG. 5. Kinetics of assembly of nucleus from monomers with concentration c through several relatively stable intermediate aggregates. For $1 \le i \le k$, f_i is the rate constant for the assembly of the $(i + 1)$th relatively stable aggregate, having concentration c_{i+1}, from the ith such aggregate, having concentration c_i, by addition of n_i monomers. b_i is the rate constant for the reverse process, and d_i is the rate constant for disintegration of the ith aggregate. The $(k + 1)$th aggregate is the nucleus, defined as the smallest aggregate to which further addition of monomers takes place one at a time and at the rate with which microtubules grow. The number concentration of these nuclei and longer microtubules is ν, and the concentration of polymer mass accumulated in them is M.

The addition of $n_i > 1$ monomers in one step at a rate proportional to c^{n_i} is the effective kinetic description which results when one is unable to time-resolve n_i rapid successive additions of a single monomer, in equilibrium with the quick decay of the highly unstable intermediate aggregates formed. Since $n_i = 1$ is allowed in Eqs. **4–6**, any degree of experimental time resolution can be captured with these equations, including perfect resolution.

$f_{k+1}c$ is the rate at which microtubules grow. We have set the backwards rates, b_i, and the destruction rates, d_i, to zero for $i \ge k + 1$, assuming microtubules can only grow. This is what we expect for microtubules stabilized with glycerol, as in ref. 4. It is what was found experimentally for microtubules stabilized with a nonhydrolyzable GTP analog (see figure 3 in ref. 11). Recently it was also demonstrated experimentally for unstabilized microtubules (12).

When self-assembly is initiated at $t = 0$, only monomers are present. Since nuclei form with difficulty, but microtubules grow rapidly, the amount of tubulin contained in nuclei and

intermediate aggregates is negligible at any time during assembly, compared to that in monomer or polymer form. If we neglect it, mass conservation gives us

$$c + M = c(0), \qquad [8]$$

where $c(0)$ is the monomer concentration at time $t = 0$.

Eq. **7** shows that M will keep growing until $c = 0$, so from Eq. **8** follows that $M(\infty) = c(0)$. Assuming the turbidity, A, is proportional[§] to the amount of polymerized tubulin, M, we have

$$A(t)/A_\infty = M(t)/M(\infty) = 1 - c(t)/c(0). \qquad [9]$$

This simple relationship is essential for our results. It means that we need not rely on results from chemical assays to determine $c(0)$ and the relationship between turbidity and polymerized tubulin. Instead we work with the relative variable $c(t)/c(0)$, and use Eq. **9** to relate this theoretical variable to the experimentally measured variable $A(t)$.

Solution to Inverse Problem

We demand that solutions to Eqs. **4–9** satisfy Eqs. **1** and **3**. This turns out to be a very strong demand. It is implemented by rewriting the generic equations (**4–7**) in terms of scaling variables, t/t_0, $c/c(0)$, $c_i/c(0)^3$, $M/M(\infty) = M/c(0)$, where t_0 [variable] $c(0)^{-3}$. This done, one demands that $c(0)$ does not appear explicitly anywhere in the equations, but only implicitly, through the scaling variables. It is this demand that forces many terms out of the equations because they do contain explicit powers of $c(0)$. It restricts the possible kinetics to just one set of equations:

$$dc_1/dt = f_0 c^6 - f_1 c^3 c_1, \qquad [10]$$

$$dc_i/dt = f_{i-1} c^3 c_{i-1} - f_i c^3 c_i \quad \text{for } 2 \le i \le k, \qquad [11]$$

$$d\nu/dt = f_k c^3 c_k, \qquad [12]$$

$$dM/dt = f_{k+1} c \nu. \qquad [13]$$

While coupled nonlinear differential equations in general are not analytically solvable, this particular set is to quite an extent (see *Analytical Solution of Model*).

Eqs. **4–7** or **10–13** are easily solved for the earliest times giving

$$A(t) \propto t^{k+2} \quad \text{for } t \simeq 0, \qquad [14]$$

i.e., a plot of $\log[A(t)/A_\infty]$ against $\log t$ displays a straight line with slope $k + 2$ at early times, independent of the initial concentration $c(0)$. The experimental turbidities of Fig. 1 were replotted in this way in Fig. 2, which shows that at early times these different time series do, indeed, all fall on straight lines with nearly the same slope. Fig. 6 shows how the value of this initial slope was determined, yielding the integer value $k + 2 = 5$ rather precisely.

We note that the size, n, of the nucleus is

$$n = n_0 + n_1 + \ldots + n_k = 3(k + 2), \qquad [15]$$

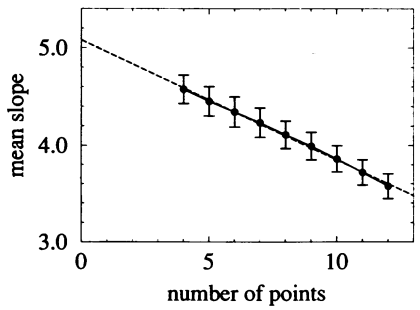

FIG. 6. Initial slope of time series in shown in Fig. 2. Straight lines were fitted to the first m points of each of the time series in Fig. 2. The average slope of those lines, and the standard error on the average, is shown here plotted against $m = 4, \ldots, 12$. Extrapolation to $m = 1$ gives our estimate, $k + 2 = 4.96 \simeq 5$, for the initial slope.

and conclude that the nucleus contains $n = 15$ monomers. This number is close to the typical number of protofilaments, 14, in self-assembled microtubules (14).

Analytical Solution of Model

Assuming only monomers are present initially, at $t = 0$ we have found a parametric solution in the form

$$t = \int_0^\tau d\tau' \gamma^{-1}(\tau'); \quad c(t) = c(0)\gamma^{2/n_0}(\tau) \qquad [16]$$

with $n_0 = 6$ and

$$\gamma(\tau) = \sum_{i=0}^{k+1} \left(\prod_{\substack{j=0 \\ j \neq i}}^{k+1} \frac{z_j}{z_i - z_j} \right) \exp(z_i \tau) \qquad [17]$$

where z_i, $i = 0, \ldots, k + 1$ are the $k + 2$ roots of the polynomial

$$z^2(z + f_1) \ldots (z + f_k) + 3 f_0 f_1 \ldots f_{k+1}. \qquad [18]$$

In mathematical terms, we have found all but one of the $k + 2$ integrals characterizing an analytical solution to Eqs. **10–13**. This solution was obtained by eliminating the dependent variables c, c_i, ν, and M in Eqs. **10–13** in favor of $\gamma = [c/c(0)]^{n_0/2}$, using Eq. **9**, and replacing the independent variable t with τ, defined by $d\tau/dt = \gamma$. This results in a $(k + 2)$th order linear differential equation for $\gamma(\tau)$ which is easily solved. The initial condition corresponding to only monomers being present at time $t = 0$, is $\gamma(0) = 1$ and $d^j\gamma/d\tau^j(0) = 0$ *for* $j = 1, \ldots, k + 1$. It is satisfied by the particular solution given in Eq. **17**; more details will appear elsewhere (unpublished data).

Eqs. **16–18** depend on f_0 and f_{k+1} only through the product $\Pi_{i=0}^{k+1} f_i$, and are furthermore invariant under permutations of $f_1, f_2, \ldots, f_k$. This is so because the turbidity, hence $M(t)$ and $c(t)$, depend only on the total length of polymer formed, and not on its distribution on microtubules, or on the concentrations of intermediate aggregates.

Eqs. **10–13** are just one set out of a class of similar sets of equations characterized by two parameters k and $n_0 = 2n_1 = 2n_2 = \ldots = 2n_k$. All these nucleation-polymerization models are analytically solvable, but for one integral. The case of $k = 0$ (nucleation in a single step from monomer to nucleus) is Oosawa's model, and fully solvable with

$$c(t) = c(0) \cosh^{-2/n_0}([f_0 f_1 n_0 c(0)^{n_0}/2]^{1/2} t). \qquad [19]$$

[§]We have considered and excluded the possibility that the initial lag in turbidity in Fig. 1 is an artifact due to short microtubules contributing less to the turbidity (13). The turbidities in Fig. 1 were measured with 350 nm light. At this wavelength, monomers as well as oligomers are transparent, while microtubules longer than the wave length—i.e., containing more than 600 monomers—contribute to the turbidity with an amount which to a good approximation is proportional to their length (see figure A2 in ref. 13). Our analysis of the turbidity time series in Fig. 1 show that at least 98% of the microtubules formed grow to a length of 350 nm in less than 2 sec—i.e., in a time that is negligible. For comparison, the origin of time is defined by the temperature "jump" initiating nucleation; it lasts 15 sec. (4).

Rate Constants

We fitted the solution for $A(t) = A_\infty[1 - c(t)/c(0)]$ to the experimental time series using the rate constants as fitting parameters (see Figs. 1 and 3). This theoretical turbidity was found by inserting Eqs. **16** and **17** with $k = 3$ and $n_0 = 6$ in Eq. **9** and fitting its four parameters, f_1, f_2, f_3, and $\Pi_{i=0}^4 f_i$ to the experimental data. Finding $f_1 = f_2 = f_3$ within insignificant differences, we chose to *assume* this identity, and fit again. The figures show the latter fit. Best fit to the data in Fig. 3 was obtained with $\Pi_{i=0}^4 f_i = 1288\ \mathrm{cm}^{15}/\mathrm{min}^5$ and $f_1 = f_2 = f_3 = 1.55\ \mathrm{cm}^3/\mathrm{min}$.

To obtain an estimate for the error on these values, we also fitted the theory to the individual time series (see Fig. 1) and averaged the parameter values obtained this way, finding $(1.2 \pm 0.3)\ 10^3\ \mathrm{cm}^{15}/\mathrm{min}^5$ and $1.0 \pm 0.9\ \mathrm{cm}^3/\mathrm{min}$, respectively. The latter values is rather uncertain, but it is not physically unrealistic. The largest initial concentration, $c(0)$, used in the experiments gives rise to a final turbidity of $0.8\ \mathrm{cm}^{-1}$. Consequently, at this initial concentration, one intermediate assembly product turns into the next one at a rate of less than 1 per minute, binding less than 3 monomers per minute. This rate should be compared with the rate at which microtubules bind monomers at the same concentration. Using $1\ \mathrm{cm}^{-1} \approx 20\ \mu\mathrm{M}$ tubulin as conversion factor between turbidity and tubulin mass (see figure 2 in ref. 4), the estimate $f_4 \approx 1\ \mu\mathrm{m}/\mathrm{min}/\mu\mathrm{M}$ (see §), and that microtubules contain about 1700 monomers per micron, we have microtubules binding approximately 27000 monomers per minute. Clearly, the creation of new microtubules is a much slower process than the growth of existing ones, even at this highest concentration studied here. Any other result would have been inconsistent with their existence. Because of the large uncertainty on the value found for $f_1 = f_2 = f_3$, the value for $f_0 f_4$, which we can extract from the value we have found for the product $f_0 f_1 f_2 f_3 f_4$, is too ill-determined to be of interest.

Discussion and Conclusion

Although the theory presented here describes the turbidity time series with precision, it is only an approximate theory. It was obtained by assuming scaling, a property that is only approximately satisfied by the experimental data. But since it is satisfied to a good approximation, the theory presented is also a good starting point for a search for a more precise theory.

As it stands, the theory fitted to the data gives $f_1 = f_2 = f_3$. This identity combined with the identity $n_1 = n_2 = n_3$ indicates that it is the *same* mechanism which stabilizes each of the intermediate assembly aggregates. A single allosteric effect involving three tubulin heterodimers could be a simple microscopic explanation of this identity. In this microscopic picture the "triplets" of tubulin heterodimers are added successively to form the nucleus containing 15 dimers. We hope that this simple result of our phenomenological model will motivate future experiments which could verify the validity of such a microscopic interpretation.

The model presented here is supported by independent experiments done at 15°C to 30°C, which measured the nucleation rate, $d\nu/dt$, at constant tubulin concentration by counting the number of individual microtubules being created, as seen through a microscope. This rate was found proportional to the tubulin concentration to the power 12 ± 2, which agrees well with the power 15 predicted by our model (15).

It is interesting to notice that the size we have found for the stable nucleus, 15 heterodimers, is very close to the typical number of protofilaments in microtubules. This suggests that the stable nucleus may be a single ring or proto-helix ("lock-washer") like those formed by the coating protein of tobacco mosaic virus (3, 16). Remarkably, γ-tubulin forms ring-like structures of size similar to our nucleus in centrosomes, where it participates in *in vivo* nucleation of microtubules, though it is not known exactly how (17). However, it has been demonstrated *in vitro* that γ-tubulin binds tightly and exclusively to the minus ends of microtubules in a saturable fashion with a stoichiometry of 12.6 ± 4.9 molecules per microtubule (18). Taken together, these experimental results indicate that a ring of γ-tubulin the size of our nucleus nucleates microtubules in centrosomes. Hence it is natural to speculate whether the nucleus discussed in the present paper has the same shape.

In conclusion, we have demonstrated that time series monitoring nonequilibrium reactions may lend themselves to a systematic mathematical analysis, and that such an analysis in some cases, such as the one presented here, may result in a unique model for the kinetics of the underlying reaction—a solution to the *inverse problem*.

We are grateful to W. A. Voter and H. P. Erickson for sending us their turbidity data and discussing them with us. We thank A. Libchaber for stimulating discussions and M. E. Fisher for many useful comments on the manuscript. This work was partially supported by the National Science Foundation (Grant PHY-9408905 and by the National Institutes of Health (Grant GM-50712). H.F. was partially supported by the Danish Natural Science Research Council (Grant 11-0244-1) and by Julie Damm's Studiefond. H.F. was on leave from the Niels Bohr Institute (Copenhagen) during the initial stages of this work.

1. Landau, L. D. & Lifshitz, E. M. (1976) *Course of Theoretical Physics* (Pergamon, New York), Vol. 1, 3rd Ed., p. 52.
2. Dyson, F. J. (1976) in *Studies in Mathematical Physics*, eds. Lieb, E. H., Simon, B. & Wightman, A. S. (Princeton Univ. Press, Princeton).
3. Voet, D. & Voet, J. G. (1990) *Biochemistry* (Wiley, New York), pp. 339–340.
4. Voter, W. A. & Erickson, H. P. (1984) *J. Biol. Chem.* **259**, 10430.
5. Oosawa, F. & Kasai, M. (1962) *J. Mol. Biol.* **4**, 10.
6. Oosawa, F. & Higashi, S. (1967) *Prog. Theor. Biol.* **1**, 79.
7. Oosawa, F. & Asakura, S. (1975) *Thermodynamics of the Polymerization of Protein* (Academic, New York), pp. 41–55.
8. Tobacman, L. S. & Korn, E. D. (1983) *J. Biol. Chem.* **258**, 3207.
9. Ferrone, F. A., Hofrichter, J. & Eaton, W. A. (1985) *J. Mol. Biol.* **183**, 611.
10. Erickson, H. P. & Pantaloni, D. (1981) *Biophys. J.* **34**, 293.
11. Hyman, A. A., Salser, S., Drechsel, D. N., Unwin, N. & Mitchison, T. J. (1992) *Mol. Biol. Cell* **3**, 1155.
12. Drechsel, D. N., Hyman, A. A., Cobb, M. H. & Kirschner, M. W. (1992) *Mol. Biol. Cell* **3**, 1141.
13. Berne, B. J. (1974) *J. Mol. Biol.* **89**, 737.
14. Chrétien, D., Metoz, F., Verde, F., Karsenti, E. & Wade, R. H. (1992) *J. Cell Biol.* **117**, 1031.
15. Fygenson, D. K., Flyvbjerg, H., Sneppen, K., Libchaber, A. & Leibler, S. (1995) *Phys. Rev.* **E51**, 5058.
16. Durham, A. C. H., Finch, J. T. & Klug, A. (1971) *Nature (London) New Biol.* **229**, 38.
17. Moritz, M., Braunfeld, M. B., Fung, J. C., Sedat, J. W., Alberts, B. M. & Agard, D. A. (1995) *J. Cell Biol.* **130**, 1149.
18. Li, Q. & Joshi, H. C. (1995) *J. Cell Biol.* **131**, 207.